Supporting Information

Fig. s1 XRD patterns of the samples LAM1 ($LaAlO_3$), LAM17 ($LaAlO_3$:0.5% Mn^{4+}, 0.1% Ge^{4+}) LAM21 ($LaAlO_3$: 0.1% Mn^{4+}, 0.9% Ge^{4+}) and LAM5 ($LaAlO_3$: 1% Mn).

Fig. s2 Persistent luminescence properties of sample LAM2, afterglow spectra recorded at 1 min and 1 h after the stoppage of irradiation. The sample was pre-irradiated by a xenon lamp for 10 min before the measurements.

Fig. s3 Thermo-luminescence and persistent luminescence curves as a function of Zn^{2+} concentration (samples LAM6, LAM7, LAM8, and LAM9), (a) Normalized thermo-luminescence curves measured at 2 min after the stoppage of irradiation. (b) Afterglow intensity monitored at 731 nm as a function of time. The samples were pre-irradiated by a xenon lamp for 10 min.

Fig. s4 Persistent luminescence properties, (a) Afterglow decay curves as a function of Ga^{3+} concentration (samples LAM10, LAM11, LAM12, and LAM13). (b) Afterglow decay curves as a function of Dy^{3+} concentration (samples LAM14, LAM15, and LAM16).The samples were pre-irradiated by a xenon lamp for 10 min.

Fig. s5 Effectiveness distinction of excitation wavelength, afterglow decay curves of sample LAM21 after irradiated by 270, 330, 400, 480, and 580 nm light for 10 min.

Fig. s6 XRD patterns of the samples GAM22 ($GdAlO_3$) and GAM23 ($GdAlO_3$: 0.1% Mn^{4+}, 0.9% Ge^{4+}).

Fig. s7 Persistent luminescence spectra and thermo-luminescence curves of sample GAM23, (a) Afterglow spectra recorded at 1 min, 30 min, and 1 h after the stoppage of irradiation. (b) Thermo-luminescence curves measured at 2 min after the stoppage of irradiation. The phosphor was pre-excited at 325 nm for 10 min.

Fig. s8 SEM image of sample GAM23.

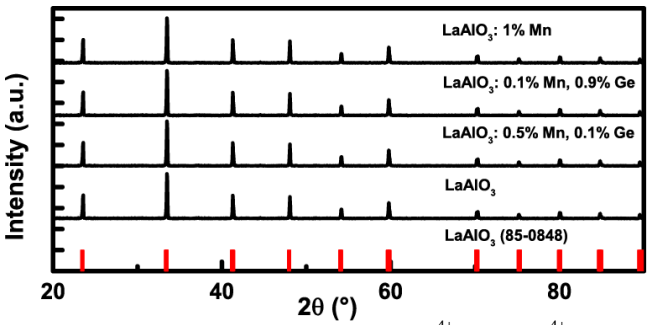

Fig. s1 XRD patterns of the samples LAM1 ($LaAlO_3$), LAM17 ($LaAlO_3$:0.5% Mn^{4+}, 0.1% Ge^{4+}) LAM21 ($LaAlO_3$: 0.1% Mn^{4+}, 0.9% Ge^{4+}) and LAM5 ($LaAlO_3$: 1% Mn).

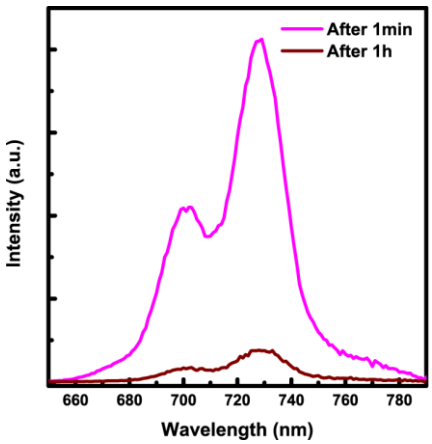

Fig. s2 Persistent luminescence properties of sample LAM2, afterglow spectra recorded at 1 min and 1 h after the stoppage of irradiation. The sample was pre-irradiated by a xenon lamp for 10 min before the measurements

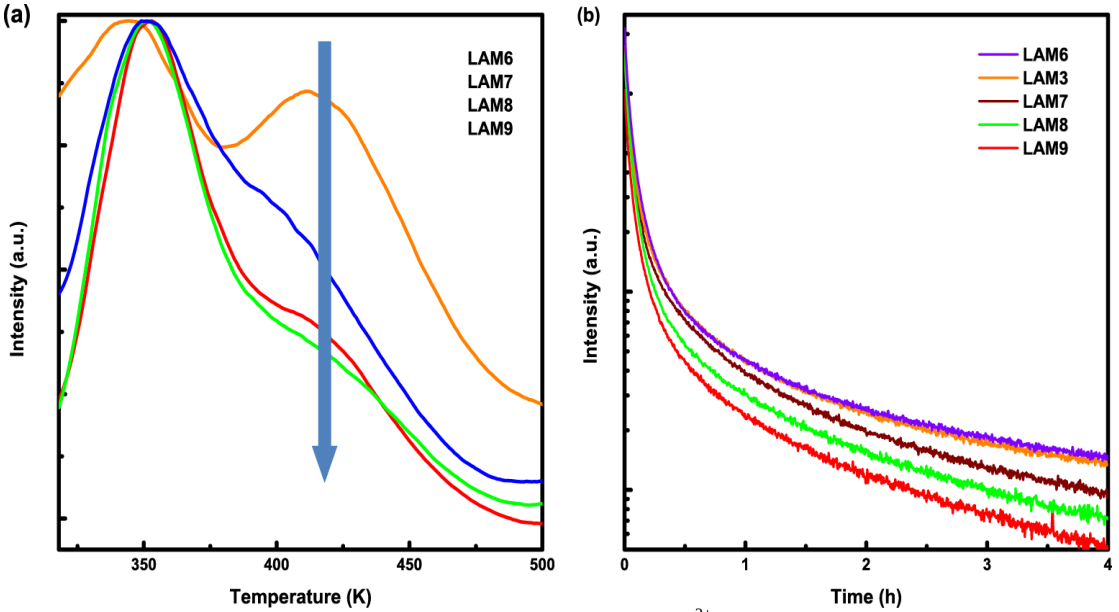

Fig. s3 Thermo-luminescence and persistent luminescence curves as a function of Zn^{2+} concentration (samples LAM6, LAM7, LAM8, and LAM9), (a) Normalized thermo-luminescence curves measured at 2 min after the stoppage of irradiation. (b) Afterglow intensity monitored at 731 nm as a function of time. The samples were pre-irradiated by a xenon lamp for 10 min.

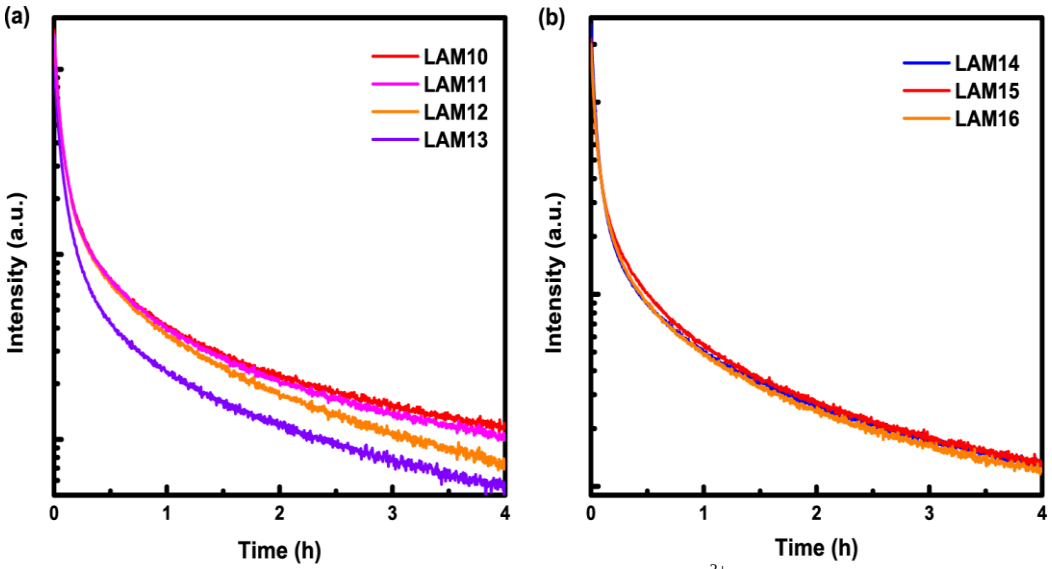

Fig. s4 Persistent luminescence properties, (a) Afterglow decay curves as a function of Ga^{3+} concentration (samples LAM10, LAM11, LAM12, and LAM13). (b) Afterglow decay curves as a function of Dy^{3+} concentration (samples LAM14, LAM15, and LAM16).The samples were pre-irradiated by a xenon lamp for 10 min.

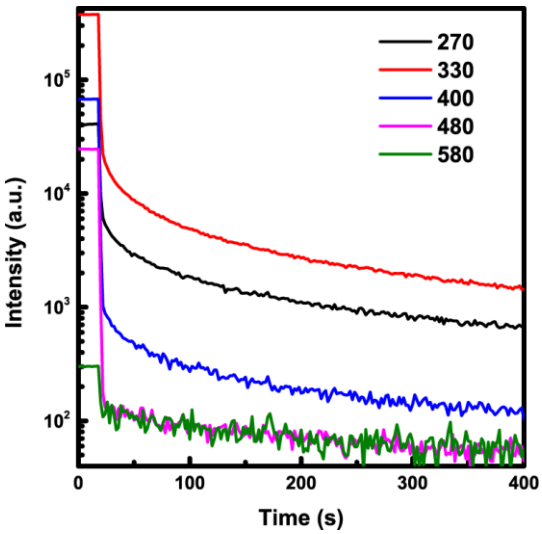

Fig. s5 Effectiveness distinction of excitation wavelength, afterglow decay curves of sample LAM21 after irradiated by 270, 330, 400, 480, and 580 nm light for 10 min.

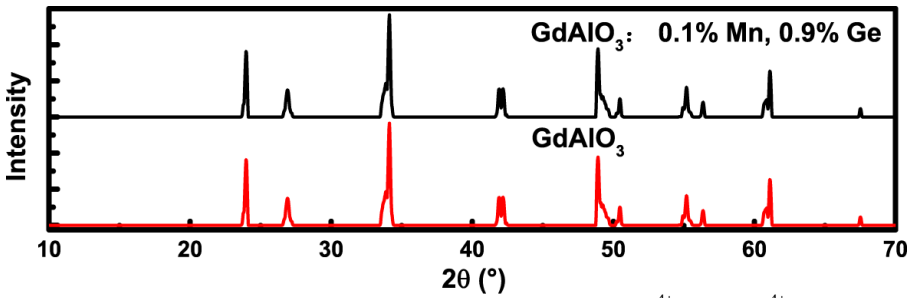

Fig. s6 XRD patterns of the samples GAM22 ($GdAlO_3$) and GAM23 ($GdAlO_3$: 0.1% Mn^{4+}, 0.9% Ge^{4+}).

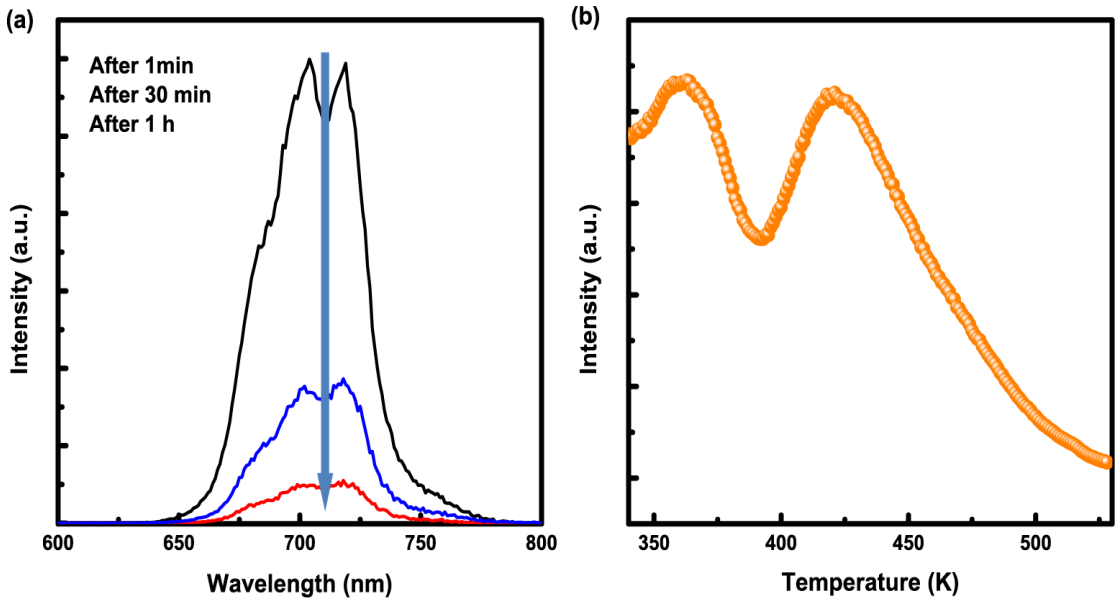

Fig. s7 Persistent luminescence spectra and thermo-luminescence curves of sample GAM23, (a) Afterglow spectra recorded at 1 min, 30 min, and 1 h after the stoppage of irradiation. (b) Thermo-luminescence curves measured at 2 min after the stoppage of irradiation. The phosphor was pre-excited at 325 nm for 10 min.

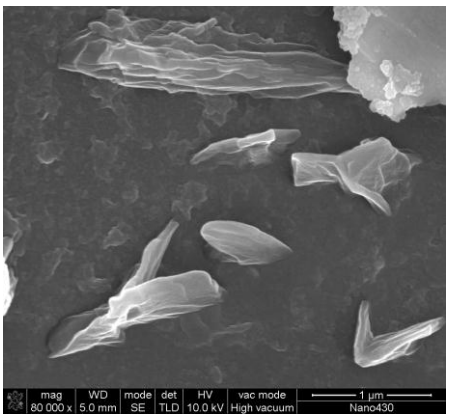

Fig. s8 SEM image of sample GAM23.